European Journal of Pharmaceutical Sciences 91 (2016) 50–63

Contents lists available at ScienceDirect

European Journal of Pharmaceutical Sciences

journal homepage: www.elsevier.com/locate/ejps

A novel hybrid drug between two potent anti-tubulin agents as a potential prolonged anticancer approach

Paolo Marchetti [a], Barbara Pavan [b,*], Daniele Simoni [a], Riccardo Baruchello [a], Riccardo Rondanin [a], Carlo Mischiati [c], Giordana Feriotto [d], Luca Ferraro [b], Lih-Ching Hsu [e], Ray M. Lee [f], Alessandro Dalpiaz [a]

[a] Department of Chemical and Pharmaceutical Sciences, University of Ferrara, 44121 Ferrara, Italy
[b] Department of Life Sciences and Biotechnology, University of Ferrara, 44121 Ferrara, Italy
[c] Department of Biomedical and Speciality Surgical Sciences, Surgery and Experimental Medicine, University of Ferrara, 44121 Ferrara, Italy
[d] Department of Morphology, Surgery and Experimental Medicine, University of Ferrara, 44121 Ferrara, Italy
[e] School of Pharmacy, College of Medicine, National Taiwan University, Taipei 10050, Taiwan
[f] Lestoni Corp., Richmond, VA 23219-155, USA

ARTICLE INFO

Article history:
Received 1 February 2016
Received in revised form 3 May 2016
Accepted 31 May 2016
Available online 01 June 2016

Keywords:
Hemiasterlin
Stilbene
Hybrid drug
Hydrolysis
Permeation
NCM460 cells

ABSTRACT

We report the design, synthesis and biological characterisation of a novel hybrid drug by conjugation of two tubulin inhibitors, a hemiasterlin derivative ***A*** (H-Mpa-Tle-Aha-OH), obtained by condensation of three non-natural amino acids, and *cis*-3,4′,5-trimethoxy-3′aminostilbene (***B***). As we have previously demonstrated synergy between ***A*** and ***B***, we used a monocarbonyl derivative of triethylene glycol as linker (***L***) to synthesise compounds ***A-L*** and ***A-L-B***; via HPLC we analysed the release of its potential hydrolysis products ***A***, ***A-L***, ***B*** and ***B-L*** in physiological fluids: the hybrid ***A-L-B*** undergo hydrolysis in rat whole blood of the ester bond between ***A*** and ***L*** (half-life = 118.2 ± 9.5 min) but not the carbamate bond between ***B*** and ***L***; the hydrolysis product ***B-L*** was further hydrolyzed, but with a slower rate (half-life = 288 ± 12 min). The compound ***A-L*** was the faster hydrolyzed conjugate (half-life = 25.4 ± 1.1 min). The inhibitory activity of the compounds against SKOV3 ovarian cancer cell growth was analysed. The IC_{50} values were 7.48 ± 1.27 nM for ***A***, 40.3 ± 6.28 nM for ***B***, 738 ± 38.5 nM for ***A-L*** and 37.9 ± 2.11 nM for ***A-L-B***. The anticancer effect of ***A-L-B*** was evidenced to be obtained via microtubule dynamics suppression. Finally, we stated the expression of the active efflux transporters P-gp (ABCB1) and MRP1 (ABCC1) in the human normal colon epithelial NCM460 cell line by reverse-transcription PCR. Via permeation studies across NCM460 monolayers we demonstrate the poor aptitude of ***A*** to interact with active efflux transporters (AET): indeed, the ratio between its permeability coefficients for the basolateral (B) → apical (A) and B → A transport was 1.5 ± 0.1, near to the ratio of taltobulin (1.12 ± 0.06), an hemiasterlin derivative able to elude AETs, and significantly different form the ratio of celiprolol (3.4 ± 0.2), an AET substrate.

1. Introduction

Some of the most important targets of anticancer drugs are the tubulin-binding sites of microtubules (Jordan and Wilson, 2004; Yue et al., 2010). Vinca alkaloid and taxane derivatives can interact with specific binding sites, while stilbene derivatives are able to interact with the *colchicine* binding site of tubulin (Gupta and Bhattacharyya, 2003; Yue et al., 2010). Interestingly, a new tubulin binding site has been identified for the hemiasterlins, a family of natural tripeptides found in marine sponges (Yue et al., 2010). Among the hemiasterlins, the synthetic derivative *taltobulin* has been characterised as a potent antitumoral agent (Zask et al., 2005).

Taltobulin can be synthesised by condensing three non-natural amino acids, although the enantioselective synthesis of one of these amino acids has been reported to be especially difficult (Nieman et al., 2003; Simoni et al., 2010). Recently, however, a versatile enantioselective means of

Abbreviations: A, H-Mpa-Tle-Aha-OH (hemiasterlin derivative obtained by condensation of three non-natural amino acids) – Mpa, *N*-(1-methyl-1-phenylethyl)-D-alanine - Tle, D-*t*.Leucine - Aha, (*2E*, *4S*)-2,5-dimethyl-4-(methylamino)-2-hexanoic acid); ***B***, *cis*-3,4′,5-trimethoxy-3′-aminostilbene; ***C***, *cis*-3,4′,5-trimethoxy-3′-hydroxystilbene (internal standard for kinetic studies); **L**, monocarbonyl-triethylene glycol; ***A-L-B***, hybrid compound obtained by coupling ***A*** with ***B***, using ***L*** as a spacer; ***A-L***, compound ***A*** linked to the spacer ***L*** using an ester function; ***L-B***, compound ***B*** linked to the spacer ***L*** using a carbamate function; AETs, active efflux transporters; ABC, ATP-binding cassette; P-gp, P-glycoprotein; MRP1, multidrug resistance-associated protein; BCRP, breast cancer resistance protein; MDR, multidrug resistance.

* Corresponding author at: Department of Life Sciences and Biotechnology, University of Ferrara, via L. Borsari, 46, 44121 Ferrara, Italy.
E-mail addresses: paolo.marchetti@unife.it (P. Marchetti), pvnbbr@unife.it (B. Pavan), daniele.simoni@unife.it (D. Simoni), riccardo.barucchello@unife.it (R. Baruchello), riccardo.rondanin@unife.it (R. Rondanin), carlo.mischiati@unife.it (C. Mischiati), giordana.feriotto@unife.it (G. Feriotto), frl@unife.it (L. Ferraro), lihchinghsu@gmail.com (L.-C. Hsu), richvain@gmail.com (R.M. Lee), dla@unife.it (A. Dalpiaz).

http://dx.doi.org/10.1016/j.ejps.2016.05.032
0928-0987/

synthesising a new class of synthetic hemiasterlins has been proposed (Hsu et al., 2012). The new hemiasterlins [an example, compound ***A*** (H-Mpa-Tle-Aha-OH) is reported in Fig. 1] have proved to be potent tubulin inhibitors, able to induce a strong synergism with cis-3,4′,5-trimethoxy-3′aminostilbene (compound ***B***, Fig. 1) (Simoni et al., 2010).

We report here the synthesis and characterisation of the hybrid compound obtained by coupling hemiasterlin ***A*** with the stilbene derivative ***B***, using the monocarbonyl derivative of triethylene glycol (***L***) as a spacer (compound ***A-L-B***, Fig. 1). The hydrolysis potential of this conjugate in physiological fluids (cell culture media, whole blood and liver homogenates) was explored, in order to determine whether it could feasibly act as a controlled release system for the hemiasterlin ***A***, whose activity is potentiated by the presence of the stilbene derivative ***B***. In order to complete the characterisation, the cytotoxic activity of both the hybrid compound and its hydrolysis products was investigated. Finally, we have evaluated the potential ability of the hemiasterlin derivative ***A*** (the main active hydrolysis product of the hybrid ***A-L-B***) to elude the active efflux transporters (AETs), that on the cell membrane are the body's first line of defence against xenobiotics. These transporters drive substrates across biological membranes, even against concentration gradients, thereby limiting xenobiotic entry into the cells. This important system of defence is generally enormously enhanced in cancer cells, in which overexpression of AETs, most notably the ATP-binding cassette (ABC) efflux transporters ABCB1 (for P-glycoprotein, P-gp), ABCC1 (multidrug resistance-associated protein, MRP1) and ABCG2 (breast cancer resistance protein, BCRP), has been implicated in multidrug resistance (MDR) (Aller et al., 2009). These ABC efflux transporters, especially ABCB1 and ABCC1, appear to be expressed in a wide variety of cancers (Dean et al., 2001; Wu et al., 2011; Pavan et al., 2014).

In order to characterise the efficacy profiles of novel anticancer drugs, it is therefore vital to consider their interactions with ABC efflux transporters (International Transporter Consortium et al., 2010). Here we report the use of normal human colon epithelial NCM460 cells as a suitable cellular model for efflux studies referred to compound ***A***. In particular, by RNA extraction and reverse- transcription PCR, NCM460 cells were shown to express the P-gp and MRP1 active efflux transporters. The permeation studies were completed by comparison of the permeability coefficients of ***A*** for the basolateral (B) → apical (A) and B → A transport with those of *celiprolol* and *taltobulin*, chosen for their ability to interact with the efflux transporters or elude them, respectively (Karlsson et al., 1993; Loganzo et al., 2003).

2. Materials and methods

2.1. Chemistry

Commercially available solvents and reagents were used without further purification. Reactions and product mixtures were routinely monitored by thin-layer chromatography (TLC) on pre-coated silica gel plates (Merck F254) using the indicated solvent systems. Flash chromatography was carried out with Merck silica gel (230–400 mesh). All the final products undergoing biological testing were purified by preparative reversed-phase HPLC [Waters Delta Prep LC 40 mm assembly column C18 (30 cm × 4 cm, 15 μm particle size)] eluted at a flow rate of 20 mL/min with mobile phase solvent A (10% CH_3CN + 0.1% TFA in

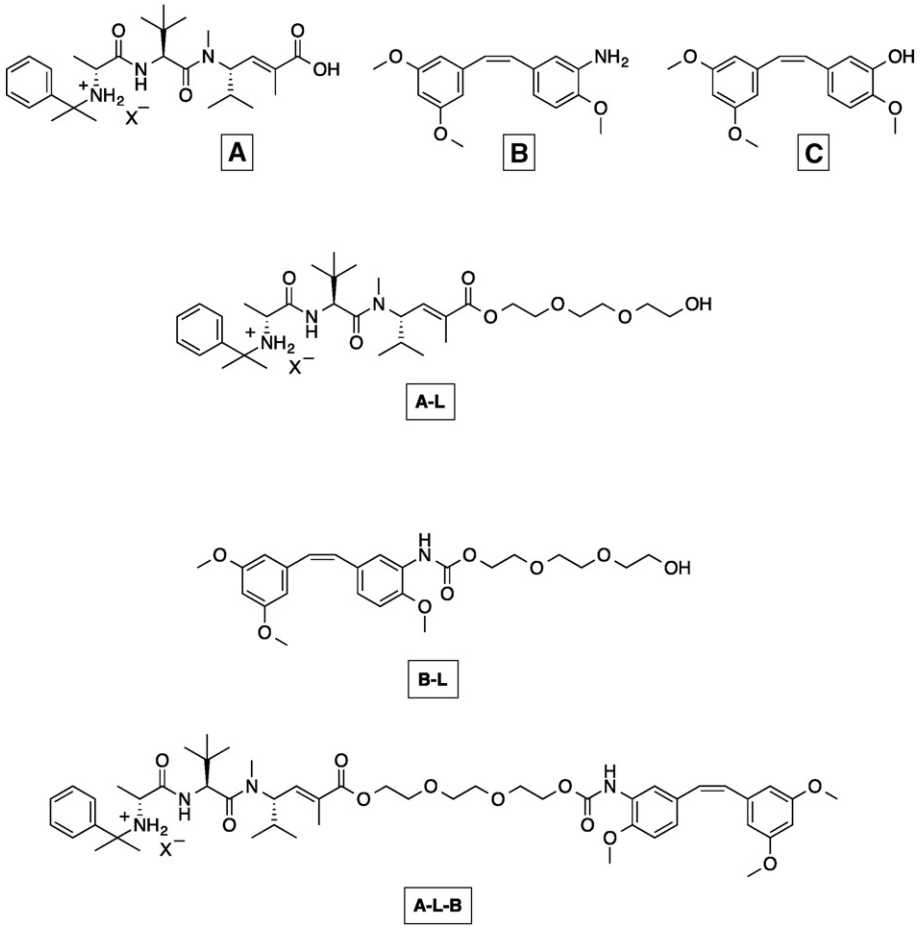

Fig. 1. Chemical formulas of the analysed hemiasterlin (***A***, ***A-L***) and stilbene (***B***, ***B-L***) derivatives and their hybrid ***A-L-B***. The stilbene derivative ***C*** was employed as an internal standard in HPLC analysis. $X^- = CF_3CO_2^-$.

H_2O v/v), and a linear gradient from 10% to 60% B (60% CH_3CN + 0.1% TFA in H_2O v/v) over 25 min. Melting points were determined on a Reichert-Kofler apparatus, and are uncorrected. NMR spectra (^1H and ^{13}C) were recorded on a Varian-Mercury Plus 400 spectrometer, and chemical shifts are given in parts per million (™) downfield from tetramethylsilane (TMS) as an internal standard; *J* values are expressed in Hz. Molecular weights of compounds were determined by mass spectrometer ESI Micromass ZMD-2000, and values are expressed as MH^+. Light petroleum (PE) refers to the fractions boiling in the range 40–60 °C. All drying operations were performed over anhydrous sodium sulfate, and evaporation was carried out using a rotary evaporator. The purity of tested compounds was determined by combustion analysis, which was conducted on a Yanagimoto MT-5 CHN recorder elemental analyser at the University of Ferrara Pharmaceutical and Chemistry Department Microanalysis Laboratory. All tested compounds yielded data within ±0.4% of calculated values.

The hemiasterlin derivative ***A***, and the compounds *cis*-3,4′,5-trimethoxy-3′-aminostilbene hydrochloride (***B***), ***B-L*** and *cis*-3,4′,5-trimethoxy-3′-hydroxystilbene (***C***) (Fig. 1), were synthesised as previously described (Simoni et al., 2009, 2010), and the new compounds as follows.

*Compound **A-L***. A solution of TEG (76.6 mg, 0.51 mmol) and DIEA (26.3 mg, 0.204 mmol) in CH_2Cl_2 (3 mL) was added dropwise to a suspension of the trifluoroacetate salt of hemiasterlin analog ***A*** (Simoni et al., 2010) (30 mg, 0.051 mmol), and PyBOP (26.5 mg, 0.051 mmol) in CH_2Cl_2 (3 mL). The reaction mixture was stirred for 24 h at room temperature before removing the solvent under reduced pressure. The product was purified first by column chromatography with (CH_2Cl_2/toluene/MeOH, 17/2.2/0.5, R_{f1}: 0.25) and then by preparative HPLC, thereby yielding compound ***A-L*** as a colourless solid (27.5 mg, 89%).
R_{f2} (CH_2Cl_2/MeOH): 0.78.
^1H NMR ($CDCl_3$): 0.76 (d, 3H, *J* = 7.2), 0.85 (d, 3H, *J* = 7.1), 0.99 (s, 9H), 1.12 (br, 3H), 1.40–1.51 (br, 8H), 1.82–1.90 (m, 1H), 1.92 (d, 3H, *J* = 1.2), 2.48–2.52 (m, 1H), 2.97 (s, 3H), 3.58–3.76 (m, 10H), 4.29–4.32 (m, 2H), 4.74 (d, 1H, *J* = 10), 5.09 (dd, 1H, *J* = 8 and 9.8), 6.67 (dd, 1H, *J* = 8 and 1.2), 7.19–7.43 (m, 5H), 8.12 (br s, 1H).
^{13}C NMR ($CDCl_3$): 13.9, 18.7, 19.5, 21.3, 21.4, 26.6, 26.7, 26.9, 30.0, 31.2, 35.3, 53.0, 54.7, 55.0, 61.8, 63.9, 69.2, 70.5, 70.7, 72.5, 110.2, 125.7, 126.8, 128.3, 132.4, 139.3, 167.7, 171.7, 173.1.
m/z: 606.709.
*Compound **A-L-B***. A solution of DIEA (0.05 mL, 0.27 mM), PyBOP (0.035 g, 0.07 mM) and compound ***B-L*** (Simoni et al., 2009) (0.035 g, 0.08 mM) in CH_2Cl_2 (3 mL) was added to a suspension of the trifluoroacetate salt of hemiasterlin analog ***A*** (Simoni et al., 2010) (0.04 g, 0.07 mM) in CH_2Cl_2 (2 mL). The mixture was stirred overnight at room temperature, and then concentrated in vacuo to give a slurry, which was purified first by column chromatography (PE/AcOEt, 1/3, R_f: 0.4) and then preparative HPLC, thereby yielding the product as a colourless solid (0.044 g, 69%).
^1H NMR ($CDCl_3$): 0.77 (d, 3H, *J* = 6.8), 0.86 (d, 3H, *J* = 6.8), 0.98 (s, 9H), 1.16 (br, 3H), 1.50 (br s, 7H), 1.83–1.91 (m, 1H), 1.92 (d, 3H, *J* = 0.8), 2.97 (s, 3H), 3.03 (m, 1H), 3.65 (s, 6H), 3.68–3.79 (m, 8H), 3.81 (s, 3H), 4.28–4.31 (m, 4H), 4.74 (d, 1H, *J* = 9.4), 5.10 (dd, 1H, *J* = 7.3 and 7.1), 6.29–6.30 (m, 1H), 6.37 (t, 1H), 6.43–6.46 (m, 5H), 6.66 (d, 1H, *J* = 8.4), 6.92 (dd, 1H; *J* = 7.3 and 0.8), 7.22–7.27 (m, 1H), 7.31–7.36 (m, 2H), 7.43–7.45 (m, 2H), 8.01 (br, 2H).
^{13}C NMR ($CDCl_3$): 14.0, 18.6, 18.9, 19.4, 25.0, 26.4, 27.4, 29.7, 29.8, 31.4, 35.8, 53.3, 55.3, 55.8, 56.2, 56.9, 63.6, 64.1, 64.3, 69.2, 69.6, 70.7, 99.7, 100.1, 106.8, 109.7, 119.3, 123.5, 126.3, 127.1, 129.2, 129.5, 129.9, 130.2, 130.5, 133, 137.8, 137.9, 160.6, 161.1, 167.4, 169.3, 171.0, 183.7.
m/z: 917.398.

2.2. Materials

Taltobulin was purchased from MedKoo Biosciences (North Carolina, USA). Trifluoroacetic acid (TFA) and celiprolol hydrochloride were obtained from Sigma-Aldrich Italia (Milan, Italy). High performance liquid chromatography (HPLC)-grade methanol, acetonitrile, ethyl acetate and water were acquired from Sigma-Aldrich, and McCoy's 5A medium and L-glutamine were purchased from Invitrogen Life Technologies (Carlsbad, CA, USA). Foetal bovine serum (FBS), Dulbecco's modified Eagle's medium (DMEM) + Glutamax, streptomycin, penicillin, and

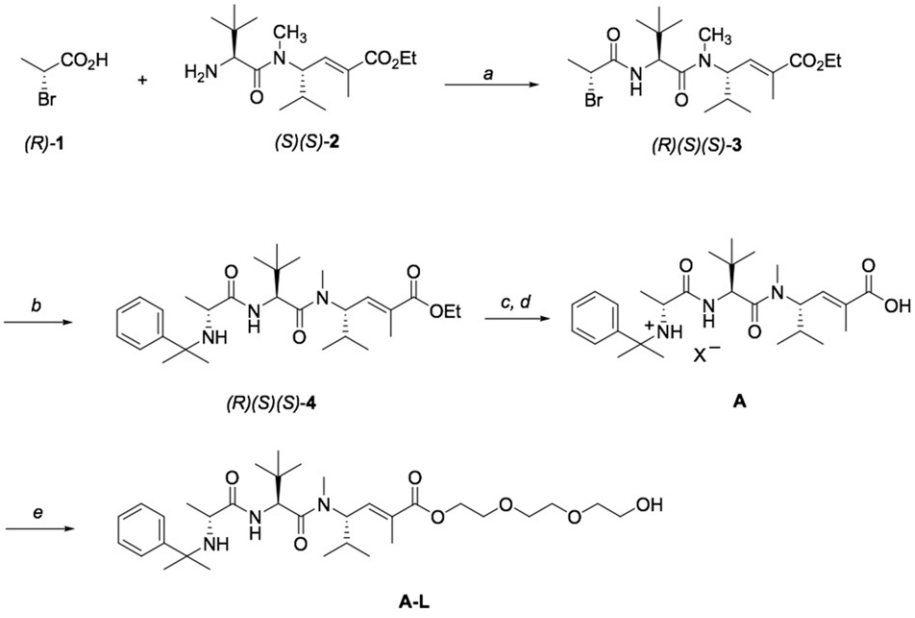

Scheme 1. Synthesis of compound ***A-L***.[a] [a]Reagent and conditions: (a) PyBOP, DIEA, CH_2Cl_2, 2 h, 76%; (b) $PhC(CH_3)_2NH_2$, Ag_2O, toluene, 1.5 h, sonication, 90%; (c) LiOH, MeOH/H_2O, 3 h, 82%; (d) H^+; (e) TEG, PyBop, DIEA, CH_2Cl_2, 24 h, 89%.

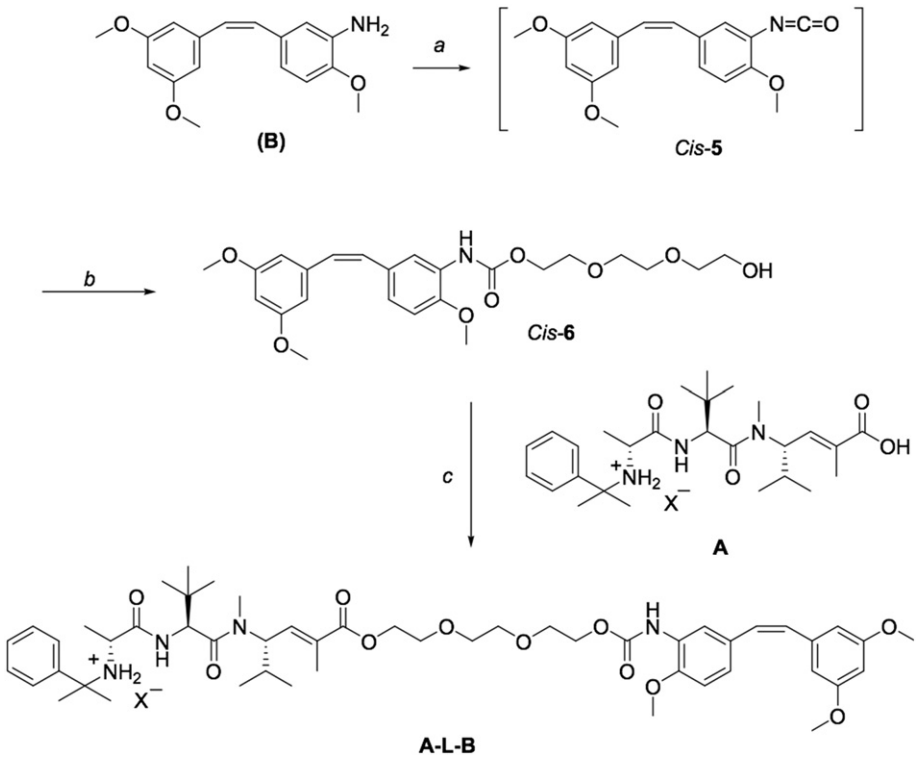

Scheme 2. Synthesis of the compound ***A-L-B***.[a] [a]Reagents and conditions: (a) Trichloromethyl chloroformate, dioxane, 60 °C, 3 h; (b) triethylene glycol, dioxane, 48 h, 78%; (c) PyBop, DIEA, CH_2Cl_2, 24 h, 69%.

phosphate-buffered saline (PBS) were obtained from Invitrogen (Life Technologies Italia, Milan, Italy).

2.3. HPLC analysis

Quantification of *taltobulin*, *celiprolol*, the hybrid compound ***A-L-B***, and its potential hydrolysis products ***A, A-L, B*** and ***B-L*** was performed by HPLC. The chromatographic apparatus consisted of a modular system (model LC-10 AD VD pump and model SPD-10A VP variable wavelength UV–Vis detector; Shimadzu, Kyoto, Japan) and an injection valve with 20 μL sample loop (model 7725; Rheodyne, IDEX, Torrance, CA, USA). Separations were performed at room temperature on a 5-μm Hypersil BDS C-18 column (150 mm × 4.6 mm *i.d.*; Alltech Italia Srl, Milan, Italy), equipped with a guard column packed with the same Hypersil material. Data acquisition and processing were performed on a personal computer using CLASS-VP Software, version 7.2.1 (Shimadzu Italia, Milan, Italy). The detector was set at 220 nm for analysis of compounds ***A*** and ***A-L*** and the hybrid ***A-L-B***, while a setting of 232 nm was used for the analysis of *celiprolol*, and 270 nm for the compounds ***B*** and ***B-L***. For the analysis of compounds ***A***, ***A-L***, ***B***, ***B-L*** and *taltobulin*, the mobile phase consisted of an isocratic mixture of water and acetonitrile in the presence of TFA 0.1% (v/v) with a ratio of 60:40 (v/v); the ratios for analysis of *celiprolol* and the hybrid ***A-L-B*** were 70:30 and 10:90 (v/v), respectively.

Kinetic analysis of the degradation of hybrid ***A-L-B*** and the release of it hydrolysis products in rat whole blood and liver homogenates were performed separately via HPLC with a mobile phase consisting of a mixture of water and acetonitrile in the presence of TFA 0.1% (v/v). Gradient profile regulation was planned and applied as follows: isocratic elution with a ratio 60:40 (v/v) for 14 min; then a 1-min linear gradient to the ratio 10:90% (v/v); followed by maintenance of the mobile phase composition at the ratio 10:90% (v/v) for 6 min. After each cycle, the column was conditioned with the ratio 60:40 (v/v) for 10 min. The flow rate was 1 mL/min, and the compound *cis*-3,4′,5-trimethoxy-3′-hydroxystilbene (***C***, Fig. 1), was employed as an internal standard for the analysis of rat blood and liver homogenate extracts.

The retention times obtained with the isocratic elutions were 4.82 min for the compounds ***A*** and ***B***, 5.30 min for the compound ***A-L***, 9.80 min for the compound ***B-L***, 12.10 min for the *internal standard* ***C***, 4.94 min for *taltobulin*, 4.50 min for *celiprolol*, and 4.60 min for the hybrid ***A-L-B***. The retention times obtained with the elution regulated by the gradient profile were the same as previously reported for the compounds ***A***, ***A-L***, ***B***, ***B-L*** and the *internal standard* ***C***, and the retention time of the hybrid ***A-L-B*** was 19.80 min. As the retention times of the compounds ***A*** and ***B*** were the same, compound ***A*** released by the hydrolysis of the hybrid ***A-L-B*** was quantified as the difference between the peak area obtained at 220 nm at 4.82 min and double the peak area obtained at 270 nm at the same retention time as the same injected sample. Indeed, compound ***A*** was found to be totally undetectable at 270 nm, whereas the mean ± S.D. of the ratio of the peak areas of compound ***B*** detected at 220 and 270 nm was 2.0 ± 0.1 in the concentration range between 5 μM and 50 μM (n = 6).

The chromatographic precisions, represented by relative standard deviations (RSD), were evaluated by repeated analysis (n = 6) of the same sample solution containing each of the examined compounds at a concentration of 10 μM. The solutes were dissolved in water, with the exception of the hybrid ***A-L-B***, which was dissolved in a 50:50 mixture of water and methanol (v/v). The RSD values ranged between 0.89% and 0.96% for all analysed compounds. Calibration curves of peak areas versus concentration (n = 9) were generated in the ranges 1 to 300 μM for the compounds ***A*** and *taltobulin*, 0.5 to 100 μM for the compounds ***A-L***, ***B*** and ***B-L***, 1 to 100 μM for the hybrid ***A-L-B***, and 0.25 to 200 μM for *celiprolol*. The calibration curves were linear (n = 9, $r > 0.996$, $P < 0.0001$) in the concentration ranges investigated.

The limits of quantification (LOQ) at a signal-to-noise ratio of 10 were 1.0 μM (5.9 ng injected) for ***A***; 0.5 μM (3.0 ng injected) for ***A-L***; 0.15 μM (0.5 ng injected) for ***B***; 0.089 μM (0.4 ng injected) for ***B-L***; 0.9 μM (9.3 ng injected) for the hybrid ***A-L-B***; 0.25 μM (0.95 ng injected) for *celiprolol*; and 0.6 μM (2.8 ng injected) for *taltobulin*. The limits of

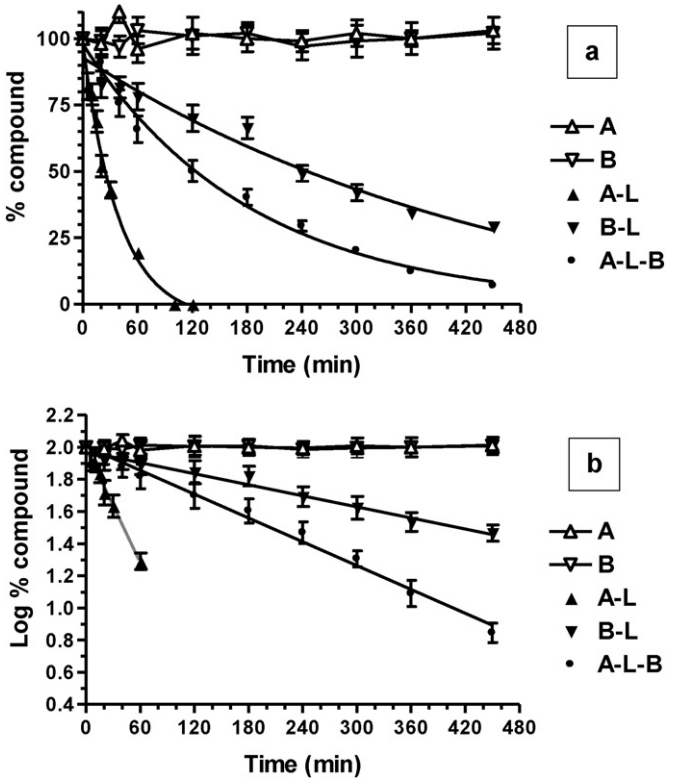

Fig. 2. [a] Degradation profiles of the compounds ***A***, ***A-L***, ***B*** and ***B-L***, and the hybrid ***A-L-B*** in rat whole blood. All values are reported as the percentage of the overall amount of incubated prodrug. [b] Semi-logarithmic plots of the degradation profiles; their linearity ($n = 9$, $r \geq 0.990$, $P < 0.0001$) evidences a degradation following an apparent first order kinetic (half-lives = 25.4 ± 1.1 min for ***A-L***, 288 ± 12 min for ***B-L*** and 118.2 ± 9.5 min for ***A-L-B***). No degradation was detected for compounds ***A*** and ***B***. Data are reported as the mean ± S.E. of three independent experiments.

detection (LOD) at a signal-to-noise ratio of 3 were 0.3 μM (1.8 ng injected) for ***A***; 0.15 μM (0.9 ng injected) ***A-L***; 0.05 μM (0.15 ng injected) for ***B***; 0.027 μM (0.12 ng injected) for ***B-L***; 0.27 μM (2.8 ng injected) for the hybrid ***A-L-B***; 0.08 μM (0.29 ng injected) for *celiprolol*; and 0.18 μM (0.84 ng injected) for *taltobulin*.

As for hydrolysis studies in different media, recovery experiments were performed by comparing the peak areas of each 25 μM compound extracted from each medium at 4 °C ($n = 3$) with those obtained by injection of an equivalent concentration of the analytes dissolved in the water-methanol mixture (50:50 v/v). The average recoveries from rat whole blood ± S.E. of 10 μM of the compounds were 91 ± 4% for ***A***; 53 ± 3% for ***A-L***; 24 ± 1% for ***B***; 95 ± 4% for ***B-L***, and 39 ± 4% for the hybrid ***A-L-B***. The average recoveries from both the cell culture medium and from rat liver homogenates (±S.E.) of 10 μM compound were ≥92 ± 4% for ***A***; ≥84 ± 3% for ***A-L***; ≥41% ± 3 for ***B***; ≥91 ± 5% for ***B-L*** and ≥54 ± 3% for the hybrid ***A-L-B***. The concentrations of these compounds were therefore referred to as peak area ratio with respect to their internal standard. The precision of this peak area ratio-based method is demonstrated by the RSD values ranging between 1.05% and 1.64% for 10 μM compounds extracted from the different incubation media at 4 °C, whose calibration curves were linear over the range 5–50 μM ($n = 6$, $r > 0.992$, $P < 0.0001$). The accuracy of the method was evaluated for each 25 μM of compound with respect to their calibration curves ($n = 6$) as relative errors ranging between −2.64% and 1.68%.

2.4. Solubility assessment

To determine their respective solubility values, an excess of compound ***A*** (8 mg/mL) or hybrid ***A-L-B*** (3 mg/mL) was added to 3 mL of water, and left to equilibrate at room temperature for 36 h under continuous stirring. After filtration, sample ***A-L-B*** was analysed by HPLC, whereas sample ***A*** was analysed after dilution to 1:100.

2.5. Kinetic analysis in culture medium

The compounds ***A***, ***A-L***, ***B*** and ***B-L*** and the hybrid ***A-L-B*** were separately incubated at 37 °C in a mixture of DMEM supplemented with 10% FBS, 50 mg/mL streptomycin, and 50 IU/mL penicillin. The kinetic analysis was performed as previously described in the case of drug incubation in plasma or rat liver homogenates (Dalpiaz et al., 2001, 2012a) The incubation phase (3 mL) was spiked with 10^{-2} M stock solutions of the compounds in DMSO in order to obtain their final concentration of 50 μM. During the experiments, the samples were shaken gently and continuously in an oscillating water bath. At regular time intervals, 100-μL aliquots of samples were taken, and immediately quenched in 300 μL of ethanol (4 °C), then adding 100 μL of 50 μM *internal standard* ***C***. After centrifugation at 13,000*g* for 10 min, 400-μL aliquots were reduced to dryness under a nitrogen stream, and re-dissolved in 150 μL of water-methanol (50:50 v/v). The solutions were then centrifuged, and 10 μL was injected into the HPLC system for sample quantification. All values were obtained as the mean of three independent incubation experiments.

Preliminary analysis performed on blank samples showed that its components did not interfere with the retention times of the compounds analysed.

2.6. Kinetic analysis in rat whole blood

The compounds ***A***, ***A-L***, ***B*** and ***B-L*** and the hybrid ***A-L-B*** were separately incubated at 37 °C in heparinised whole blood obtained from different rats (male Wistar, Harlan SRC, Milan, Italy) weighing 200–250 g.

All procedures involving the rats were performed in accordance with the guidelines issued by the Italian Ministry of Health (D.L. 116/92 and D.L. 111/94-B), the Declaration of Helsinki, and the Guide for the Care and Use of Laboratory Animals as adopted and promulgated by the National Institute of Health (Bethesda, Maryland, USA). The experimental design has been approved by the Local Ethics Committee (University of Ferrara, Ferrara, Italy). All efforts were made to reduce the number of animals and their suffering.

The kinetic analysis was performed as previously described (Dalpiaz et al., 2001). Three millilitres of whole blood was spiked with compound solutions to yield a final concentration of 50 μM, obtained by adding 5 μL of 10^{-2} M stock solution in DMSO for each millilitre incubated. During the experiments, the samples were shaken gently and continuously in an oscillating water bath. At regular time intervals, 100-μL aliquots of samples were taken, and immediately quenched in 500 μL of ice cold water, then adding 50 μL of 10% sulfosalicylic acid and 100 μL of 100 μM *internal standard* ***C***. Sulfosalicylic acid was added in order to induce the denaturation and precipitation of the proteins in the incubation media. Differently from sodium hydroxide, used for the same purpose, sulfosalicylic acid does not induce the hydrolysis of the prodrugs (Dalpiaz et al., 2001). The samples were extracted twice with 1 mL of water-saturated ethyl acetate, and, after centrifugation, the organic layer was reduced to dryness under a nitrogen stream. Two hundred microlitres of a water and methanol mixture (50:50 v/v) was added, and, after centrifugation, 10 μL was injected into the HPLC system. All values were obtained as the mean of three independent incubation experiments. Preliminary analysis performed on blank samples showed that its components did not interfere with the retention times of the compounds analysed.

2.7. Preparation of rat liver homogenates

The livers of male Wistar rats were immediately isolated after their decapitation, washed with ice-cold saline solution, and homogenized

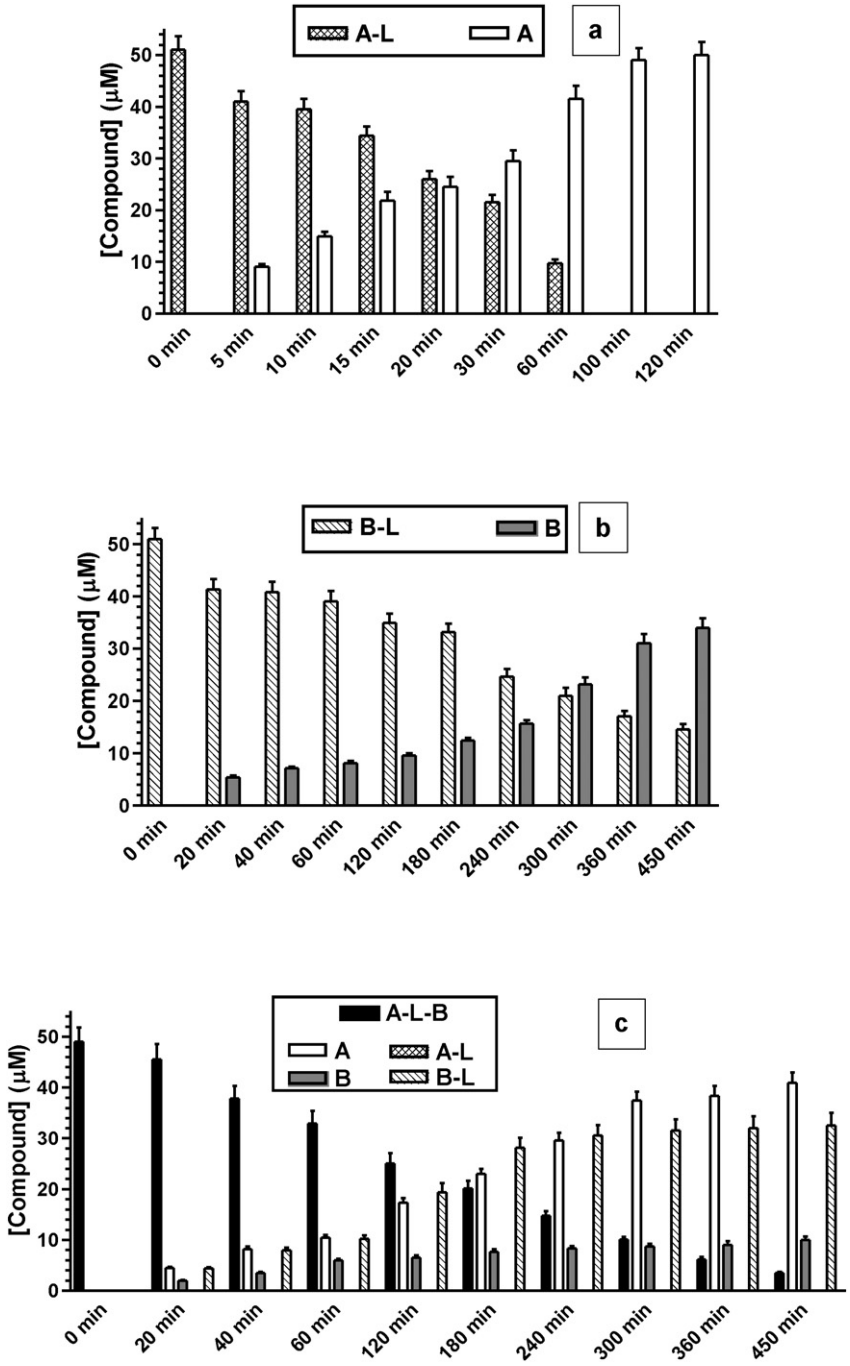

Fig. 3. Degradation profiles of the compounds ***A-L*** [a], ***B-L*** [b] and ***A-L-B*** [c], with the corresponding appearance profiles of their hydrolysis products in rat whole blood. All the values are reported as the concentrations of compounds detected in the blood during time and as the mean ± S.E. of three independent experiments.

in 4 volumes (w/v) of TrisHCl (50 mM, pH 7.4, 4 °C) with a Potter-Elvehjem apparatus (Vetrotecnica, Padua, Italy). The supernatant obtained after centrifugation (2000*g* for 10 min at 4 °C) was decanted off and stored at −80 °C before being used in kinetics studies. The total protein concentration in the tissue homogenate was determined using the Lowry procedure (Lowry et al., 1951), and was found to be 31.8 ± 1.3 μg of protein/μL.

2.8. Kinetic analysis in rat liver homogenates

The compounds ***A***, ***A-L***, ***B*** and ***B-L*** and the hybrid ***A-L-B*** were separately incubated at 37 °C in 3 mL of rat liver homogenates, resulting in a final concentration of 50 μM, obtained by adding 15 μL of 10^{-2} M stock solution in DMSO. The kinetic analysis was performed as previously described (Dalpiaz et al., 2012a). During the experiments, the samples were shaken gently and continuously in an oscillating water bath. At regular time intervals, 100-μL aliquots of samples were taken, and immediately quenched in 300 μL of ethanol (4 °C). After addition of 100 μL of 100 μM *internal standard* ***C*** and centrifugation at 13,000*g* for 10 min, 400-μL aliquots were reduced to dryness under a nitrogen stream, and re-dissolved in 150 μL of water-methanol mixture (50:50 v/v), prior to centrifugation and injection of 10 μL into the HPLC system. All values were obtained as the mean of three independent incubation experiments. Preliminary analysis performed on blank samples showed

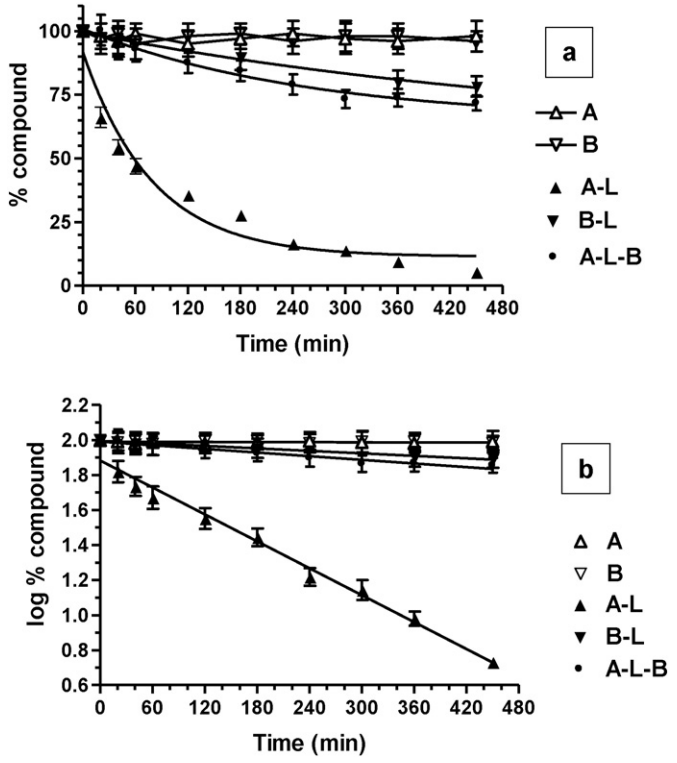

Fig. 4. [a] Degradation profiles of the compounds ***A***, ***A-L***, ***B***, ***B-L*** and hybrid ***A-L-B*** in rat liver homogenates. All values are reported as a percentage of the overall amount of incubated prodrug. [b] Semi-logarithmic plots of the degradation profiles; their linearity ($n = 9$, $r \geq 0.973$, $P < 0.0001$) evidences a degradation following an apparent first order kinetic (half-life of ***A-L*** $= 118.0 \pm 7.2$ min). The degradation of both compounds ***B-L*** and hybrid ***A-L-B*** was less than 30% during 8 h of incubation. No degradation was detected for compounds ***A*** and ***B***. Data are reported as the mean ± S.E. of three independent experiments.

that its components did not interfere with the retention times of the compounds analysed.

2.9. Kinetics calculations

The computer program GraphPad Prism (GraphPad, San Diego, CA) was used to calculate the half-lives of the compounds showing first-order kinetic decay on an exponential decay plot of their concentration versus incubation time. The same software was then used for linear regression of the corresponding semi-logarithmic plots. The quality of fit was determined by evaluating the correlation coefficients (r) and P values.

2.10. Pharmacological measurements

An ovarian cancer cell line SKOV3 was used to compare the growth-inhibitory effect of the hybrid compound ***A-L-B*** with that of ***A***, ***A-L***, and ***B***. SKOV3 cells were maintained in McCoy's 5A medium supplemented with 10% foetal bovine serum and 1.5 mM L-glutamine, and seeded in a 96-well plate at 2500–3500 cells/well one day before drug treatment. Cells were then treated with various concentrations of compounds for 48 h, and cell viability was measured by MTT assay. Half-maximal inhibitory concentrations (IC_{50}) were then calculated using Scientist software. Experiments were performed in triplicate, and data were presented as mean ± S.E. of two to five independent experiments.

2.11. Flow cytometry analysis

SKOV3 cells were treated with 100 nM of compound ***A***, ***B*** or ***A-L-B*** for 6 to 48 h, and harvested by trypsinisation. Cells were then fixed for at least 30 min in 75% ethanol at −20 °C, and subjected to propidium iodide (PI) staining and flow cytometry analysis. At least 10,000 cells from each sample were analysed using CellQuest Pro software (BD Biosciences, San Jose, CA).

2.12. Cell culture

The human-derived non transformed colon mucosa NCM-460 cells, kindly provided by Dr. Enzo Spisni (Dept. of Biological, Geological and Environmental Sciences, University of Bologna, Italy) were grown in DMEM/Glutamax culture medium supplemented with 10% foetal bovine serum (FBS), 100 U/mL penicillin and 100 μg/mL streptomycin at 37 °C in a humidified atmosphere of 95%, with 5% CO_2. For maximum viability, NCM460 cells were passaged at pre-confluent densities twice a week in fresh and spent growth medium in a 1:1 ratio. NCM460 cells were used between passages 29 and 39 in this study.

2.13. RNA extraction and reverse-transcription PCR

Total RNA was isolated from 10 million cells as follows. The cells were lysed in 1 mL of TRIzol Reagent (Invitrogen, Carlsbad, CA, USA) by pipetting. After incubation of the homogenized samples for 5 min at room temperature, 0.2 mL of chloroform was added. The samples were stirred vigorously, and then centrifuged at 12,000*g* for 15 min at 4 °C. The RNA was precipitated from the aqueous phase at room temperature by adding 0.5 mL of isopropanol, and centrifuging at 12,000*g* for 10 min at 4 °C. The RNA pellet was washed once with 75% ethanol, and then air-dried and dissolved in diethyl pyrocarbonate (DEPC)-treated water. The RNA concentration was determined by measuring the optical absorbance at 260 nm. Reverse transcription was performed from 2 μg of total RNA using ImProm-II™ (Promega, Madison, WI, USA) and a mixture of oligo-dT and random primers in a final volume of 20 μL. To perform the PCR reactions, 0.5-μL aliquots of cDNA and the following forward and reverse gene-specific primers were used: ABCB1, *Homo sapiens* ATP-binding cassette, sub-family B, member 1 (5′-ATG TTT CCG GTT TGG AGC CT-3′/5′-TCC TTC CAA TGT GTT CGG CA-3′); ABCC1, *Homo sapiens* ATP-binding cassette, sub-family C, member 1 (5′-CCT GAA GGT GGA CGA GAA CC-3′/5′-TGT GCC TGA GAA CGA AGT CC-3′); ABCG2, *Homo sapiens* ATP-binding cassette, sub-family G, member 2 (variant 1, 5′-CTC CCA TCG TGA CCT CCA GC-3′/5′-TCA TTG GAA GCT GTC GCG GG-3′; variant 2, 5′-GGG TAA TCC CCA GGC CTC TA-3′/5′-TGA GAT TGA CCA ACA GAC CAT CA-3′). In order to prevent amplification from genomic DNA, the forward and reverse primers were designed on exons separated by a long intronic sequence; briefly, 25 μL of PCR mixture, containing 0.4 μM primers, 2.5 mM $MgCl_2$, 0.4 mM deoxynucleoside triphosphates, and 0.2 μL DyNAzyme II DNA Polymerase (Finnzymes, Espoo, Finland) were amplified using a T100 thermal cycler (Bio-Rad Laboratories, Hercules, CA). The thermal cycler conditions included initial denaturation for 30 s, and then 28 cycles of 95 °C for 10 s; annealing at 62 °C for 30 s; and at 72 °C for 45 s. PCR products were separated on 2% agarose gel, stained with ethidium bromide, and examined under UV light with the aid of a Gel Doc 1000 Documentation System (Bio-Rad Laboratories, Hercules, CA). In order to confirm the quality of cDNA, amplification of human actin, GAPDH and HMBS housekeeping genes was performed in parallel PCR reactions. Negative controls (no template cDNA) were also run on every experimental plate to assess specificity and to rule out contamination. In order to demonstrate the specificity of amplification, ABCB1 and ABCC1 PCR products were sequenced in both forward and reverse directions by using the PCR primers and the complete PCR sequence was determined. Then, sequences were aligned to the human genomic plus transcript database by web access to the BLASTN program (Zhang et al., 2000) at National Center for Biotechnology Information, NIH. The alignments were optimized by using the megablast algorithm that permits to retrieve highly similar sequences. By using the ABCB1 PCR sequence as query, only the sequences NM_000927.4, NC_018918.2 and NC_000007.14

produced significant alignments (100% of identity), respectively corresponding to the mRNA of Homo sapiens ATP-binding cassette, sub-family B (MDR/TAP), member 1 (ABCB1) gene and to genomic sequences of the Homo sapiens chromosome 7 containing the ABCB1 gene. Similarly, the ABCC1 PCR sequence produced significant alignments with the sequences NM_004996.3, NC_018927.2, NC_000016.10 and NT_187607.1, the first was correspondent to the Homo sapiens ATP-binding cassette, sub-family C (CFTR/MRP), member 1 (ABCC1), mRNA and the others to the genomic sequences of the Homo sapiens chromosome 16 containing the ABCC1 gene.

2.14. Differentiation of NCM460 cells into polarised monolayers

Differentiation to NCM460 cell monolayers was performed using a modified version of the method reported by Dalpiaz et al. (2012a). Briefly, after two passages, confluent NCM460 cells were seeded at a density of 10^5 cells/mL in a 1:1 ratio of fresh and spent culture medium, housed in 12-well Millicell inserts (Millipore, Milan, Italy) made of polyethylene terephthalate (PET) filter membranes of surface area 1.12 cm^2 and pore size of 1.0 μm. Filters were pre-soaked for 24 h with fresh culture medium, and then the upper compartment (apical, A) received 400 μL of the diluted cells, whereas the lower (basolateral, B) received 2 mL of the medium in the absence of cells. A half volume of the culture medium in the upper and lower compartments was replaced with fresh medium every two days. The integrity of the cell monolayers was monitored by measuring the transepithelial electrical resistance (TEER) by means of a voltmeter (Millicell-ERS; Millipore, Milan, Italy). The resistance measured was multiplied by the area of the filter to obtain an absolute value of TEER, expressed in $\Omega \cdot cm^2$. The background resistance of blank inserts not plated with cells, around 35 $\Omega \cdot cm^2$, was deducted from each value. The homogeneity and integrity of the cell monolayers were also monitored by phase-contrast microscopy.

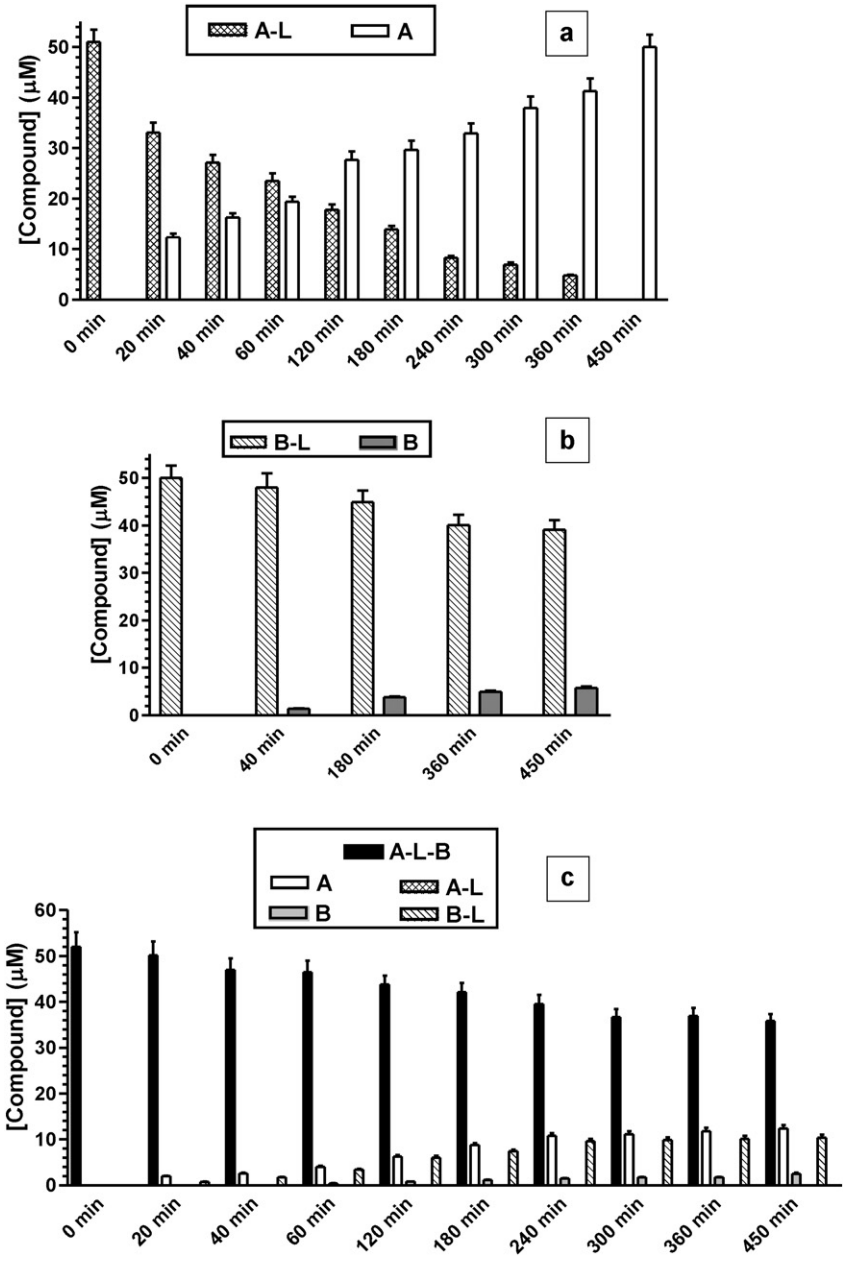

Fig. 5. Degradation profiles of the compounds ***A-L*** [a], ***B-L*** [b] and ***A-L-B*** [c], with the corresponding appearance profiles of their hydrolysis products in rat liver homogenates. All the values are reported as the concentrations of compounds detected in the homogenate during time and as the mean ± S.E. of three independent experiments.

Based on these parameters, cell monolayers reached confluence and epithelial polarisation after 6 days, and monolayers with a stable TEER value of 180 ± 11 $\Omega \cdot cm^2$ were used in permeation experiments, after the medium in both the apical and basolateral compartments had been replaced with fresh low-serum medium (1% FBS) and left for 24 h.

2.15. Permeation studies across cell monolayers

Permeation experiments were performed in triplicate in both the apical-to-basolateral (A → B) and basolateral-to-apical (B → A) directions. To this end, solutions of compound ***A***, *celiprolol* and *taltobulin* were separately prepared in PBS containing 5 mM glucose at a concentration of 100 μM, obtained by adding 5 μL of $2 \cdot 10^{-2}$ M stock solution in DMSO for each millilitre incubated. The fresh low-serum media-cultured monolayers of NMC460 cells were removed from both the A and B sides of the inserts, and both sides were washed twice with pre-warmed PBS. During transport experiments, the Millicell systems were continuously swirled on an orbital shaker (100 rpm) at 37 °C. For the A → B permeation studies, 0.4 mL of compound ***A***, *celiprolol*, or *taltobulin* solution was added to the apical side at time t = 0, and the inserts were placed in a cell culture plate whose basolateral compartment was pre-filled with 2 mL of pre-warmed PBS containing 5 mM glucose. At the pre-established time points, the inserts were removed and transferred to a new well-plate containing fresh PBS with glucose. The contents of the basolateral compartment were collected after insert removal, and 10-μL aliquots of filtered (0.45 μm) samples were immediately injected into the HPLC apparatus. For the B → A permeation studies, at time t = 0, 2 mL of compound ***A***, *celiprolol*, or *taltobulin* solutions were placed on the basolateral side of Millicell inserts whose apical side contained 0.4 mL of fresh PBS with glucose. At the predetermined time points, the apical samples were removed and replaced with fresh PBS containing glucose. The collected apical samples were immediately filtered (0.45 μm) and injected (10 μL) into the HPLC apparatus. TEER values were monitored before and after each experiment. Permeation studies were also conducted using cell-free inserts under the same conditions described above as control. All values obtained were the means of three independent experiments.

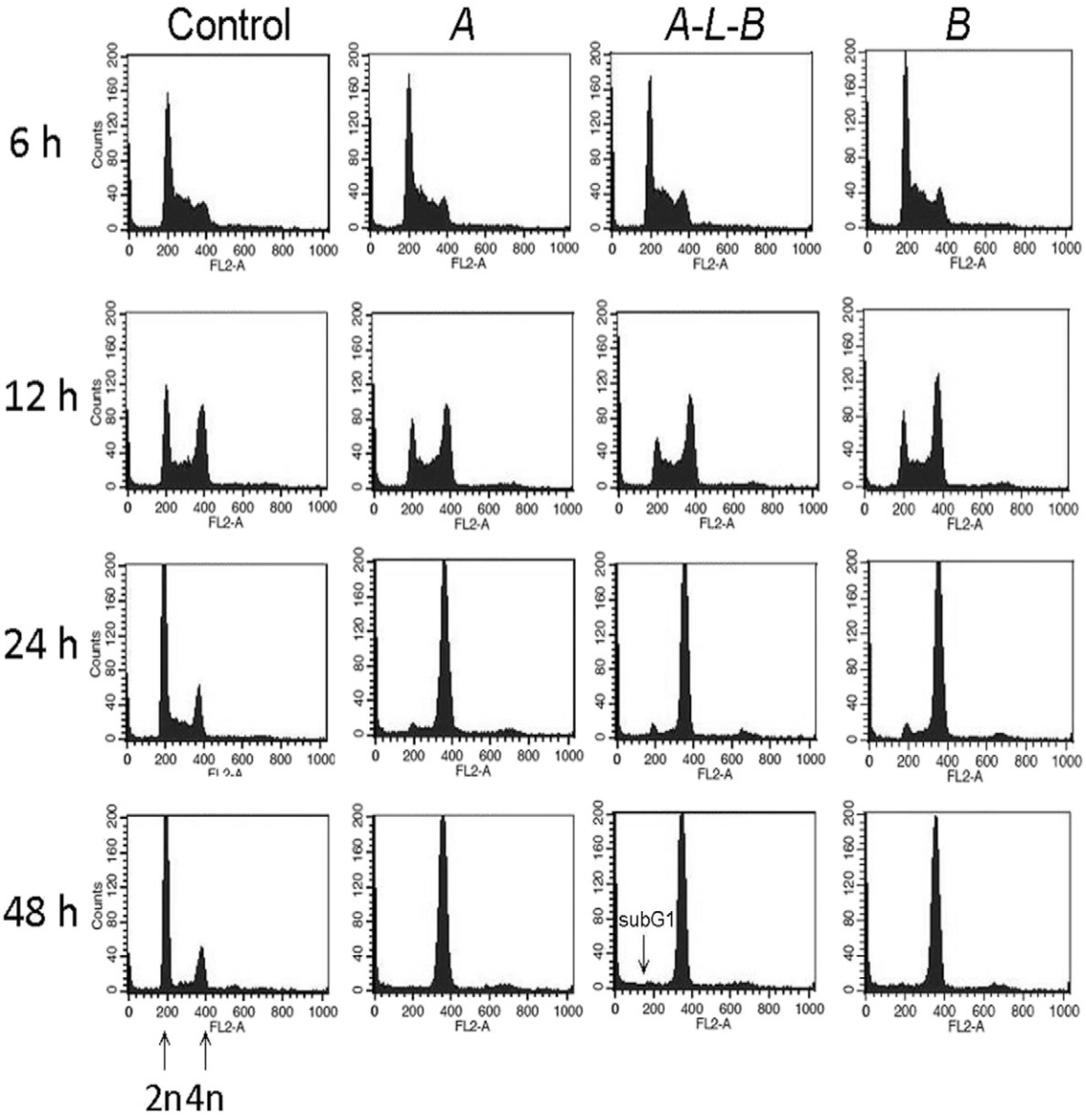

Fig. 6. Cell cycle arrest induced by the compounds ***A***, ***A-B-L*** and ***B***. SKOV3 cells were treated with DMSO (Control) or 100 nM of each compound for 6 to 48 h and harvested for flow cytometric analysis. The hybrid compound ***A-B-L*** was as potent as compounds ***A*** and ***B*** in inducing mitotic arrest and apoptosis.

Apparent permeability coefficients (P_{app}) of the analysed compounds were calculated according to the following equation (Artursson and Karlson, 1991; Pal et al., 2000; Raje et al., 2003):

$$P_{app} = \frac{\frac{dc}{dt}V_r}{S_A C_o} \quad (1)$$

where P_{app} is the apparent permeability coefficient in cm/min; dc/dt (μM/min) is the flux of drug across the filters, calculated as the linearly regressed slope through linear data; V_r is the volume in the receiving compartment (apical = 0.4 mL; basolateral = 2 mL); S_A is the diffusion area (1.13 cm^2); and C_0 is the initial compound concentration in the donor chamber at t = 0.

The permeabilities were determined for the filters alone (P_f), and for the filters covered with cells (P_t). The apparent permeability coefficients (P_E) of the cell monolayer were then calculated as follows (Raje et al., 2003; Yee, 1997):

$$\frac{1}{P_E} = \frac{1}{P_t} - \frac{1}{P_f} \quad (2)$$

2.16. Statistical analysis

Statistical comparisons of permeability coefficients and cumulative concentrations obtained from the transport studies were made by one-way ANOVA or Student's *t*-test (GraphPad Prism). $P < 0.05$ was considered statistically significant. GraphPad Prism was employed for linear regression of the cumulative amounts of the compounds in the receiving compartments of the Millicell systems. The quality of fit was determined by evaluating the correlation coefficients (r) and P values.

3. Results and discussion

3.1. Chemistry

It is known that hemiasterlins are capable of influencing both the *vinca alkaloid* and *colchicine*-binding sites of tubulin (Nunes et al., 2005; Ravi et al., 2005; Kuznetsov et al., 2009), and we have previously demonstrated that the free compound ***A*** and the stilbene derivative ***B*** synergize with each other in their anti-microtubule activity (Hsu et al., 2012). As conjugation between active drugs can bring about their controlled release through hydrolysis processes occurring in physiological fluids (Dalpiaz et al., 2012b), this study proposes a conjugation of the compounds ***A*** and ***B*** in order to investigate the potential antitumor activity of the conjugate or its ability to be prodrug of the parent compounds. Indeed, a hybrid approach in which at least one component targets tubulin is known to improve the clinical outcome of anticancer therapies (Breen and Walsh, 2010). Due to the issue that the water solubility of the stilbene derivative ***B*** is very poor (<1 mg/mL) (Simoni et al., 2009) a hydrophilic spacer ***L*** (triethylenglicole) was used for conjugation with the hemiasterlin derivative ***A***. The solubilities of compound ***A*** and the hybrid ***A-L-B*** by us detected in water were 7.7 ± 0.5 mM (4.5 ± 0.03 mg/mL) and 14.5 ± 0.7 μM (0.015 ± 0.001 mg/mL), respectively. It is encouraging to note that the poor water solubility of ***A-L-B*** indicates this hybrid as a good candidate for encapsulation studies, further to the development of nanoparticulate formulations able to induce selective targeting of tumoral tissues (Pavan et al., 2014).

The synthesis and the cytotoxic activities of the compounds ***A***, ***B*** and ***B-L*** have been reported previously (Hsu et al., 2012; Roberti et al., 2003; Simoni et al., 2009, 2010). We completed a series of potential hydrolysis products of the hybrid ***A-L-B*** along with the synthesis of compound ***A-L***, to characterise its cytotoxicity and potential aptitude to be hydrolyzed in physiologic fluids.

Single diastereoisomers of compounds ***A-L*** and ***A-L-B*** were therefore synthesised, respectively, as depicted in Schemes 1 and 2. The synthesis

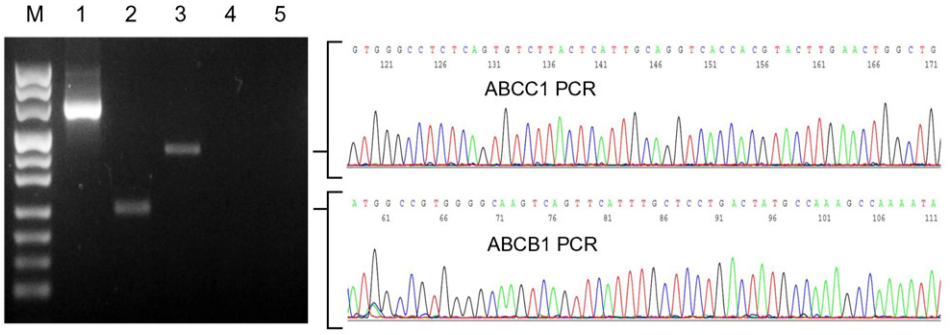

ABCC1 PCR sequence

CCTGAAGGTGGACGAGAACCAGAAGGCCTATTACCCCAGCATCGTGGCCAACAGGTGGCTGGCCGTGCGGCTGGAGTGTG
TGGGCAACTGCATCGTTCTGTTTGCTGCCCTGTTTGCGGTGATCTCCAGGCACAGCCTCAGTGCTGGCTTG**GTGGGCCTCT**
CAGTGTCTTACTCATTGCAGGTCACCACGTACTTGAACTGGCTGGTTCGGATGTCATCTGAAATGGAAACCAACATCGTGG
CCGTGGAGAGGCTCAAGGAGTATTCAGAGACTGAGAAGGAGGCGCCCTGGCAAATCCAGGAGACAGCTCCGCCCAGCAG
CTGGCCCCAGGTGGGCCGAGTGGAATTCCGGAACTACTGCCTGCGCTACCGAGAGGACCTGGACTTCGTTCTCAGGCACA

ABCB1 PCR sequence

ATGTTTCCGGTTTGGAGCCTACTTGGTGGCACATAAACTCATGAGCTTTGAGGATGTTCTGTTAGTATTTTCAGCTGTTGTCTT
TGGTGCC**ATGGCCGTGGGGCAAGTCAGTTCATTTGCTCCTGACTATGCCAAAGCCAAAATA**TCAGCAGCCCACATCATCAT
GATCATTGAAAAAACCCCTTTGATTGACAGCTACAGCACGGAAGGCCTAATGCCGAACACATTGGAAGGA

Fig. 7. Expression of multi-drug resistance channel genes in NCM460 cells. The RNA isolated from NCM460 cells was retro-transcribed, specific cDNAs for the beta-actin (lane 1), ABCB1 (lane 2) and ABCC1 (lane 3) genes were amplified by PCR and analysed by agarose gel electrophoresis. As negative control, the un-reverted RNA was amplified in the presence of primers specific for ABCB1 (lane 4) and ABCC1 (lane 5). M = pUC mix marker 8 (Fermentas). PCR products were sequenced to confirm the specificity of amplification and the complete sequences obtained have been reported in the lower side. Regions recognized by the PCR primers have been underlined.

of hemiasterlin congener ***A*** represented the most challenging synthetic sequence; its key step was an Ag_2O-promoted nucleophilic substitution (Maran, 1993; D'angeli et al., 1995; Marchetti et al., 1997) on the chiral non-racemic precursor 2-bromo-derivative (*R*)(*S*)(*S*)-**3**, which was achieved via condensation of 2-bromoacid (*R*)-**1** with dipeptide (*S*)(*S*)-**2**. Bromine displacement by 2-phenyl-2-propanamine yielded tripeptide-ester (*R*)(*S*)(*S*)-**4**, which possessed the desired regio- and stereochemistry to produce hemiasterlin derivative ***A*** via the subsequent hydrolysis with LiOH. The carboxyl group of ***A*** was then reacted with triethylene glycol by standard procedures to yield the corresponding ester ***A-L***.

The amino-stilbene ***B*** was quite easily prepared, as previously described and illustrated in Scheme 2, via a Wittig reaction between the opportune phosphonium salt and aldehyde. The *cis*-stereoisomer yield was lower than that of the *trans*-stereoisomer (1:2 ratio), but, being the only active isomer, it was readily isolated by flash chromatography. Reaction with trichloromethyl chloroformate derivatised the amino group of ***B*** to isocyanate (*Cis*-**5**), which was condensed, without purification, with triethylene glycol to obtain the carbamate *Cis*-**6** (Simoni et al., 2010). The hybrid compound ***A-L-B*** was then produced by esterification of ***A*** at the C-terminus with hydroxyl group of *Cis*-**6**.

3.2. Hydrolysis and stability studies

We have firstly evaluate the potential hydrolysis pattern of the hybrid compound ***A-L-B*** in different media, namely cell culture medium, rat whole blood, and rat liver homogenates. To this end it was necessary to detect and quantify not only the hybrid compound ***A-L-B***, but also its potential hydrolysis products, ***A***, ***A-L***, ***B*** and ***B-L***, in all incubation media. In order to do so, we developed an efficacious HPLC-UV method of analysis employing a reverse-phase C-18 HPLC column and a mobile phase constituted by a mixture of water and acetonitrile in the presence of TFA following a gradient profile. No interference from the culture medium, whole blood or liver homogenate components was observed, and the gradient profile therefore allowed us to quantify, on the same HPLC chromatograms in all incubation media investigated, both the hybrid ***A-L-B*** and its hydrolysis products ***A***, ***A-L***, ***B*** and ***B-L***. Thanks to isocratic elution we were also able to use one HPLC chromatogram to quantify the compounds ***A-L*** and ***B-L*** and their potential hydrolysis products, ***A*** and ***B*** respectively, in all incubation media investigated.

First we verified that neither ***A-L-B*** nor any of its potential hydrolysis products were degraded by a mixture of DMEM supplemented with FBS, streptomycin and penicillin, a medium employed for growth inhibition studies of several cancer cell lines (Simoni et al., 2009). Although neither ***A*** nor ***B*** incubated at 37 °C in either rat whole blood or rat liver homogenates showed signs of degradation after 8 h (Figs. 2 and 4), under the same experimental conditions the compounds ***A-L***, ***B-L*** and the hybrid ***A-L-B*** all did, exhibiting different half-lives according to the compound and type of incubation medium. As shown in Fig. 2, the half-lives in rat whole blood of compounds ***A-L***, and ***B-L***, and the hybrid ***A-L-B*** were 25.4 ± 1.1 min, 288 ± 12 min and 118.2 ± 9.5 min, respectively. These degradation profiles were indicative of pseudo first-order kinetics, as confirmed by the linear patterns of corresponding semi-logarithmic plots ($n = 9$, $r \geq 0.990$, $P < 0.0001$), suggesting that the degradation of ***A-L*** and ***B-L*** was governed by hydrolysis. This was confirmed by the appearance in incubation media of their hydrolysis products, ***A*** and ***B***, respectively, in a time-dependent fashion (Fig. 3a and b). Specifically, after 100 min of incubation in rat whole blood, the compound ***A-L*** appeared to have been completely hydrolyzed, whereas the incubation of ***B-L*** for 450 min resulted in the degradation of about 70% of its starting concentration, alongside the appearance of a corresponding amount of its hydrolysis product ***B***. As reported in Fig. 3c, the degradation of the hybrid ***A-L-B*** was accompanied by the appearance of the compounds ***A*** and ***B-L***, whose patterns increased over time. As no compound ***A-L*** was detected, this indicates that the urethane bond between ***B*** and the *linker* was not hydrolyzed in rat whole blood, whereas the ester bond between ***A*** and the *linker* was. Indeed, as evidenced in Fig. 3c, the amounts of ***A*** released over time in rat whole blood appeared to correspond with the amount of the hybrid ***A-L-B*** degraded. Hence we can deduce that the appearance of ***B*** during incubation of ***A-L-B*** in rat whole blood (Fig. 3c) was caused by the hydrolysis of ***B-L***, released during the degradation of the hybrid compound.

In rat liver homogenates, the compounds ***A-L***, ***B-L*** and the hybrid ***A-L-B*** all showed hydrolysis patterns similar to those observed in rat whole blood, albeit characterised by significantly lower rates of degradation. Indeed, as reported in Fig. 4, during 8 h of incubation less than 30% of the compounds ***B-L*** and ***A-L-B*** were degraded, whereas more than 95% of compound ***A-L*** was degraded, showing a half-life of 118.0 ± 7.2 min. Fig. 5 reveals that the degradation of these compounds was due to hydrolysis, and, as observed in rat whole blood, that only the ester bond between ***A*** and the *linker* of the hybrid ***A-L-B*** was hydrolyzed. To summarize, the compound with the fastest rate of hydrolysis

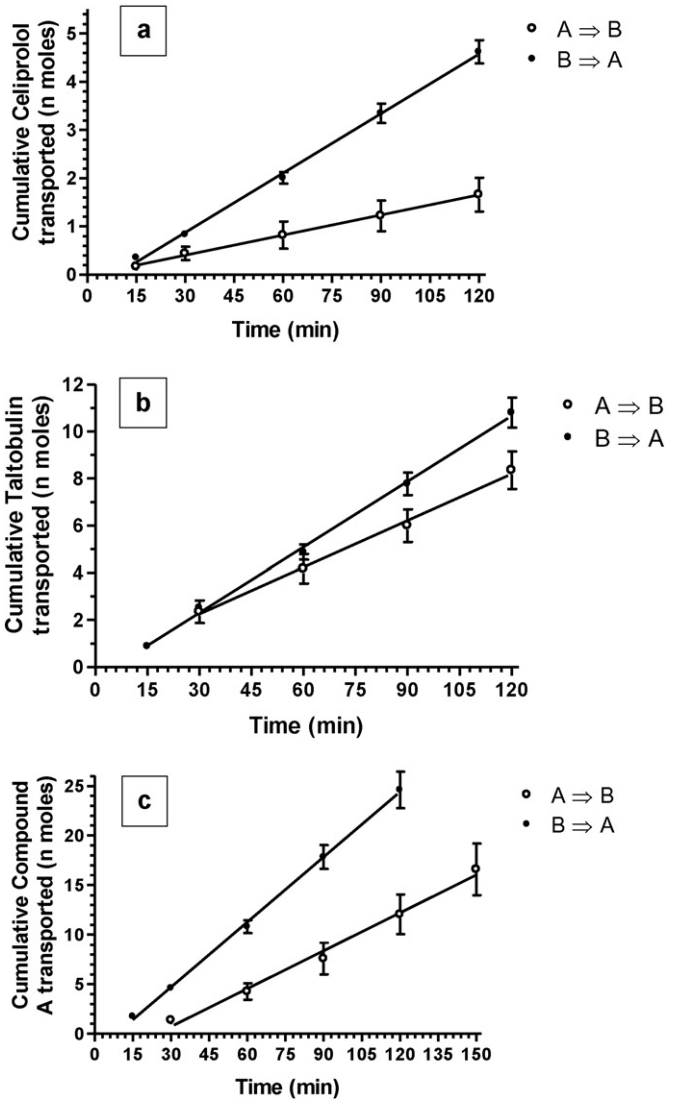

Fig. 8. Permeation kinetics of 100 μM *celiprolol* [a], *taltobulin* [b], and compound ***A*** [c] across the Millicell filters covered by monolayers obtained by NCM460 cells. The permeations were analysed from the apical to basolateral compartments (A → B) and from the basolateral to apical compartments (B → A). In all cases analysed, the cumulative amounts in the receiving basolateral compartment were linear across 120 min or 150 min ($r \geq 0.995$, $P \leq 0.002$). All data are reported as mean ± S.E. of three independent experiments.

was ***A-L*** in which the drug and the linker are joined by an ester bond, whereas the hydrolysis of conjugate ***B-L*** was very slow, indicating that endogenous enzymes have difficulty hydrolyzing the urethane bond between the ***B*** and ***L***. This pattern was confirmed by the hydrolysis profile of the hybrid compound ***A-L-B***, in which only the ester bond between ***A*** and ***L*** moieties was hydrolyzed to any great extent, at rates intermediate between those of ***A-L*** and ***B-L***. These results are supported by the observation that the biodegradation of poly(ester-urethane)s in blood appears to be mainly due to breakage of their ester bonds, whereas the hydrolysis of urethane bonds is dependent on the linking agents used in their synthesis (Liu et al., 2009). They also suggest that ***A-L-B*** may be a useful means of achieving the prolonged release of compounds ***A*** and ***B*** in physiological fluids. However, further in-vivo studies are necessary to corroborate the current in vitro kinetic data.

3.3. Pharmacological measurements

Previous studies indicated that the IC_{50} values of compound ***A*** range from 10 to 20 nM (Simoni et al., 2010; Hsu et al., 2012) and compound ***B*** from 15 to 30 nM in UCI-101 human ovarian cancer cells (Simoni et al., 2009; Hsu et al., 2012), whereas compound ***B-L*** is inactive and has an IC_{50} value greater than 10,000 nM in the same cell line (Simoni et al., 2009), probably due to its inability to fit into the *colchicine*-binding pocket (Simoni et al., 2009). Here we compared the potencies of compounds ***A***, ***B***, ***A-L*** and ***A-L-B*** in another human ovarian cancer cell line, SKOV3, treated with various concentrations of the compounds for 48 h and measured by MTT assay. We obtained IC_{50} values of 7.48 ± 1.27 nM for compound ***A*** (n = 5), 40.3 ± 6.28 nM for compound ***B*** (n = 2), 738 ± 38.5 nM for compound ***A-L*** (n = 3), and 37.9 ± 2.11 nM for compound ***A-L-B*** (n = 2). This shows that, like ***B-L***, ***A-L*** was much less potent with respect to compound ***A***. Taken together with the above, these results suggest that the presence of a *linker* may block the activity of both compounds ***A*** and ***B***, by compromising the fit with the hemiasterlin binding site. Furthermore, these data suggest that the *linker* is not hydrolyzed in the in vitro cell culture system. In contrast, the hybrid compound ***A-L-B*** was much more potent than ***A-L*** or ***B-L***, displaying an IC_{50} very close to that of compound ***B*** under cell culture conditions. It may be that further investigation of the spacer length may enable modulation of the activity of the ***A-B*** conjugates. Moreover, further investigations on the potential hydrolysis of ***A-L-B*** in the SKOV3 cells may indicate the contributions of the various compounds to its pharmacologic activity.

Tubulin inhibitors exert their anticancer effect via suppression of microtubule dynamics, which leads to mitotic arrest and apoptosis. To determine the cell cycle effect of the hybrid compound ***A-L-B***, SKOV3 cells were treated with 100 nM of ***A-L-B*** for 6, 12, 24 and 48 h, and subjected to PI staining and flow cytometry analysis. Compounds ***A*** and ***B*** were included for comparative purposes. Results shown in Fig. 6 indicate that the hybrid compound ***A-L-B*** was as potent as compounds ***A*** and ***B*** in inducing M phase arrest and apoptosis, which, at 48 h, involved approximately 80% of G2/M cells and 17% of the subG1 population.

3.4. Millicell permeation studies

The results above reported indicate that the hybrid ***A-L-B*** is hydrolyzed in physiologic fluids, allowing the release of the compound ***A***, that exhibits potent anti-microtubule activity, being a parent compound of *taltobulin*, a potent anti-cancer agent (Simoni et al., 2010; Hsu et al., 2012). However, is vital to determine whether, like its parent compound (Loganzo et al., 2003; Zask et al., 2005), ***A*** is able to elude AET systems, whose overexpression by cancer cells induces MDR (Pavan and Dalpiaz, 2011; Pavan et al., 2014). To this end, we set out to study the potential interaction of ***A*** with the active efflux transporters on human NCM460 cells. We evidenced that, after confluence in Millicell systems, these cells acquire functional polarisation, thereby acting as an epithelial barrier (Valerii et al., 2015; Ferretti et al., 2015). Therefore, we used NCM460 cells as a pharmacological barrier-based approach of human origin, where investigating interaction of drugs with efflux transporters. We preferred to use NCM460 cells with respect to other consolidate models, such as Caco-2 cells, because changes in growth characteristics (monolayers/multilayers) are known to occur in Caco-2 cell line, due to the loose of contact inhibition and polarisation in transformed cell (Rothen-Rutishauser et al., 2000).

First we conducted control experiments to provide evidence that the NCM460 cell monolayer is can be a useful model for drug transport studies, initially by RT-PCR analysis of the expression of active efflux transporters P-gp, MRP1 and BCRP in this cell line (Fig. 7). This analysis was performed on total RNA using specific primers that recognize the genes ABCB1 (P-gp), ABCC1 (MRP1), and ABCG2 – variant 1 and variant 2 – (BCRP). Since amplification products were obtained only for the genes ABCB1 and ABCC1, we were able to deduce that NCM460 cells express the P-gp and MRP1 active efflux transporters. The expression and activity of P-gp transporters in NCM460 cells was verified by permeation experiments using the P-gp substrate *celiprolol* (Karlsson et al., 1993). In particular, transport studies were performed in both the apical-to-basolateral (A → B) and basolateral-to-apical (B → A) directions after cell cultures reached the confluence on parallel sets of Millicell well plates with similar TEER values (180 ± 11 Ω cm^2). The permeation profiles of *celiprolol* across the Millicell filters covered with monolayers of NCM460 cells are reported in Fig. 8a, where it is shown that the cumulative amounts of *celiprolol* (nmol) in the receiving compartments have a linear profile over 120 min in all cases ($r \geq 0.999$, $P \leq 0.001$), indicating constant permeation conditions within this range of time. A linear profile has been also observed for permeations across the filters alone (data not shown). The slopes of the linear fits were used to calculate the permeability coefficients (P_t and P_f), which were in turn used to calculate, as per eq. 2, the apparent permeability coefficients (P_E) of *celiprolol* specific for the cell monolayers, which are reported in Table 1. The P_E values for A → B and B → A transport of *celiprolol* were $2.95 \pm 0.06 \times 10^{-4}$ and $9.98 \pm 0.56 \times 10^{-4}$ cm/min, respectively, indicating that the permeation rate of this drug from the basolateral to the apical compartments was roughly 3.5 times higher than its permeation rate in the opposite direction ($P < 0.001$), in accordance with the expression of the active efflux transporter P-gp in NCM460 cell monolayers. Thus, even if NCM460 cells are known to show untransformed

Table 1
Permeability coefficients (P_E) (×10–5 cm/min) of *celiprolol*, *taltobulin* and compound ***A*** transported by the millicell system NCM460 cells monolayer. The values were obtained from coefficients P_t and P_f, as in Eq. (2). Coefficients refer to transport from the apical compartment (A) to the basolateral compartment (B) and vice versa. The ratio between the P_E values for the basolateral (B) → apical (A) and B → A transport are reported.

Compound	A → B	B → A	Ratio (B → A)/(A → B)
Celiprolol	2.95 ± 0.06	9.98 ± 0.56[a]	3.4 ± 0.2
Taltobulin	6.21 ± 0.28	6.96 ± 0.24	1.12 ± 0.06[c]
Compound ***A***	5.28 ± 0.44	7.96 ± 0.37[b]	1.5 ± 0.1[c,d]

[a] $P < 0.001$ as compared to P_E value of *celiprolol* transported from A to B.
[b] $P < 0.01$ as compared to P_E value of *compound **A*** transported from A to B.
[c] $P < 0.001$ as compared to ratio value of *celiprolol*.
[d] $P > 0.05$ as compared to ratio value of *taltobulin*.

properties, we observed that they express the same secretion activity (basal-to-apical direction) of a model drug-effluxed such as celiprolol as well as it can be observed in Caco-2 cell line, a well-established system for permeation studies (Karlsson et al., 1993).

We then performed identical transport studies with *taltobulin*, a reference drug able to elude the P-gp transporter (Loganzo et al., 2003). The permeation profiles of this drug from the apical to basolateral compartments (A → B) and vice versa are reported in Fig. 8b, and cumulative amounts (nmol) in both showed a linear profile over 120 min in all cases ($r \geq 0.998$, $P \leq 0.002$), indicating constant permeation conditions within this range of time. In this case, however, the P_E values for A → B and B → A transport were $6.21 \pm 0.28 \times 10^{-4}$ and $6.96 \pm 0.24 \times 10^{-4}$ cm/min, respectively (Table 1), indicating a very similar permeation rate in both directions ($P > 0.05$), and suggesting that this drug was effectively eluding the AET systems, as reported in the literature (Nieman et al., 2003). Together, the data reported in Table 1 and Figs. 7–8 provide compelling evidence that NCM460 cell monolayers could represent a useful model for drug transport studies.

Hence we applied this model to study the transport of compound ***A***, whose permeation profiles from the apical to basolateral compartments (A → B) and vice versa are reported in Fig. 8c. In all cases the receiving compartments showed cumulative amounts (nmol) exhibiting a linear profile across 120 min or 150 min ($r \geq 0.995$, $P < 0.001$), indicating constant permeation conditions during these ranges of time. In this case, the P_E values for A → B and B → A transport were $5.28 \pm 0.44 \times 10^{-4}$ and $7.96 \pm 0.37 \times 10^{-4}$ cm/min, respectively (Table 1), i.e., the permeation rate of compound ***A*** in a basolateral to apical direction was about 1.5 times higher than the reverse ($P < 0.01$), demonstrating its behavioural similarity to *taltobulin*, as opposed to *celiprolol*. Indeed, analysis of the ratios between the P_E values for the basolateral → apical and apical → basolateral directions were 3.4 ± 0.2 for *celiprolol*, 1.12 ± 0.06 for *taltobulin*, and 1.5 ± 0.1 for compound ***A*** (Table 1), the former being statistically higher than the latter two ($P < 0.001$). As the P_E ratios for *taltobulin* and compound ***A*** were very similar ($P > 0.05$), compound ***A*** appeared as a weaker AET substrate than celiprolol in this experiment.

As multidrug resistance (MDR) is often the major obstacle to the success of cancer chemotherapy, it is currently a crucial issue. This phenomenon is brought about by several factors, but among these overexpression of ABC drug transporters by cancer cells appears to be the most influential. Indeed, a considerable amount of experimental data supports a role of ABC transporters, in particular ABCB1 and ABCC1, in acquired MDR (Monti, 2007). The NCM640 cell monolayers revealed that compound ***A*** is a substrate of ABC transporters weaker than celiprolol, suggesting that it may exert its anticancer effect with very poor AET-mediated MDR phenomena.

4. Conclusions

The hybrid compound ***A-L-B*** obtained by the conjugation of the hemiasterlin derivative ***A*** and the stilbene derivative ***B*** using triethylenglicole (***L***) as a spacer, is able to induce a sustained release of the compound ***A*** by hydrolysis of its ester bond with ***L***, in rat whole blood. The hydrolysis of the urethane bond between ***B*** and ***L*** has been observed only for the compound ***B-L*** and it induced a slow release in rat whole blood of the compound ***B***. Easily synthesised by a versatile enantioselective approach, unlike other antitumoral members of the hemiasterlin family, compound ***A*** is known to synergize its anticancer activity with the stilbene derivative ***B***. The hybrid compound ***A-L-B*** showed anticancer activity with a potency similar to that of compound ***B*** and an order of magnitude lower than that of compound ***A***. On the other hand, the presence of the spacer ***L*** in compounds ***A-L*** and ***B-L*** induced a drastic decrease of their anticancer activity. We have demonstrated that the main hydrolysis product of ***A-L-B***, i.e. the hemiasterlin derivative ***A***, is a weak substrate of active efflux proteins, suggesting its poor aptitude to induce MDR phenomenon. Furthermore, the poor water solubility of ***A-L-B*** indicates this hybrid as a good candidate for nanoparticle encapsulation studies, potentially being suitable for targeted delivery and prolonged release of compound ***A***, a potentially efficacious and selective anticancer drug.

Acknowledgements

Support from the University of Ferrara (F72I15000470005) in the frame of the project FAR2014 is gratefully acknowledged.

References

Aller, S.G., Yu, J., Ward, A., Weng, Y., Chittaboina, S., Zhuo, R., Harrell, P.M., Trinh, Y.T., Zhang, Q., Urbatsch, I.L., Chang, G., 2009. Structure of P-glycoprotein reveals a molecular basis for polyspecific drug binding. Science 323, 1718–1722.

Artursson, P., Karlson, J., 1991. Correlation between oral absorption in humans and apparent drug permeability coefficients in human intestinal epithelial (Caco-2) cells. Biochem. Biophys. Res. Commun. 175, 880–885.

Breen, E.C., Walsh, J.J., 2010. Tubulin-targeting agents in hybrid drugs. Curr. Med. Chem. 17, 609–639.

Dalpiaz, A., Scatturin, A., Menegatti, E., Bortolotti, F., Pavan, B., Biondi, C., Durini, E., Manfredini, S., 2001. Synthesis and study of 5′-ester prodrugs of N^6-cyclopentyladenosine, a selective A_1 receptor agonist. Pharm. Res. 18, 531–536.

Dalpiaz, A., Paganetto, G., Pavan, B., Fogagnolo, M., Medici, A., Beggiato, S., Perrone, D., 2012a. Zidovudine and ursodeoxycholic acid conjugation: design of a new prodrug potentially able to bypass the active efflux transport systems of the central nervous system. Mol. Pharm. 9, 957–968.

Dalpiaz, A., Cacciari, B., Vicentini, C.B., Bortolotti, F., Spalluto, G., Federico, S., Pavan, B., Vincenzi, F., Borea, P.A., Varani, K., 2012b. A novel conjugated agent between dopamine and an A_{2A} adenosine receptor antagonist as a potential anti-parkinson multitarget approach. Mol. Pharm. 9, 591–604.

D'angeli, F., Marchetti, P., Bertolasi, V., 1995. Stereoselective substitution in 2-bromo amides in the presence of Ag^+ or Ag_2O. J. Organomet. Chem. 60, 4013–4016.

Dean, M., Hamon, Y., Chimini, G., 2001. The human ATP-binding cassette (ABC) transporter superfamily. J. Lipid Res. 42, 1007–1017.

Ferretti, V., Dalpiaz, A., Bertolasi, V., Ferraro, L., Beggiato, S., Spizzo, F., Spisni, E., Pavan, B., 2015. Indomethacin co-crystals and their parent mixtures: does the intestinal barrier recognize them differently? Mol. Pharm. 12, 1501–1511.

Gupta, S., Bhattacharyya, B., 2003. Antimicrotubular drugs binding to vinca domain of tubulin. Mol. Cell. Biochem. 253, 41–47.

Hsu, L.C., Durrant, D.E., Huang, C.C., Chi, N.W., Baruchello, R., Rondanin, R., Rullo, C., Marchetti, P., Grisolia, G., Simoni, D., Lee, R.M., 2012. Development of hemiasterlin derivatives as potential anticancer agents that inhibit tubulin polymerization and synergize with a stilbene tubulin inhibitor. Invest. New Drugs 30, 1379–1388.

International Transporter Consortium, Giacomini, K.M., Huang, S.M., Tweedie, D.J., Benet, L.Z., Brouwer, K.L., Chu, X., Dahlin, A., Evers, R., Fischer, V., Hillgren, K.M., Hoffmaster, K.A., Ishikawa, T., Keppler, D., Kim, R.B., Lee, C.A., Niemi, M., Polli, J.W., Sugiyama, Y., Swaan, P.W., Ware, J.A., Wright, S.H., Yee, S.W., Zamek-Gliszczynski, M.J., Zhang, L., 2010. Membrane transporters in drug development. Nat. Rev. Drug Discov. 9, 215–236.

Jordan, M., Wilson, L., 2004. Microtubules as a target for anticancer drugs. Nat. Rev. Cancer 4, 253–265.

Karlsson, J., Kuo, S.M., Ziemniak, J., Artursson, P., 1993. Transport of celiprolol across human intestinal epithelial (Caco-2) cells: mediation of secretion by multiple transporters including P-glycoprotein. Br. J. Pharmacol. 110, 1009–1016.

Kuznetsov, G., TenDyke, K., Towle, M.J., Cheng, H., Liu, J., Marsh, J.P., Schiller, S.E., Spyvee, M.R., Yang, H., Seletsky, B.M., Shaffer, C.J., Marceau, V., Yao, Y., Suh, E.M., Campagna, S., Fang, F.G., Kowalczyk, J.J., Littlefield, B.A., 2009. Tubulin-based antimitotic mechanism of E7974, a novel analogue of the marine sponge natural product hemiasterlin. Mol. Cancer Ther. 8, 2852–2860.

Liu, Q., Cheng, S., Li, Z., Xu, K., Chen, G.Q., 2009. Characterization, biodegradability and blood compatibility of poly[(*R*)-3-hydroxybutyrate] based poly(ester-urethane)s. J. Biomed. Mater. Res. A 90, 1162–1176.

Loganzo, F., Discafani, C.M., Annable, T., Beyer, C., Musto, S., Hari, M., Tan, X., Hardy, C., Hernandez, R., Baxter, M., Singanallore, T., Khafizova, G., Poruchynsky, M.S., Fojo, T., Nieman, J.A., Ayral-Kaloustian, S., Zask, A., Andersen, R.J., Greenberger, L.M., 2003. HTI-286, a synthetic analogue of the tripeptide hemiasterlin, is a potent antimicrotubule agent that circumvents P-glycoprotein-mediated resistance in vitro and in vivo. Cancer Res. 63, 1838–1845.

Lowry, O.H., Rosebrough, N.J., Farr, A.L., Randall, R.J., 1951. Protein measurement with the folin phenol reagent. J. Biol. Chem. 193, 265–275.

Maran, F., 1993. Electrochemical and stereochemical investigation on the mechanism of the decay of 2-halo amide anions. The intermediacy of aziridinones. J. Am. Chem. Soc. 115, 6557–6563.

Marchetti, P., D'Angeli, F., Bertolasi, V., 1997. Stereoselective synthesis of neutral and cationic 2-heterocyclically substituted propanamides. Tetrahedron Asymmetry 8, 3837–3842.

Monti, E., 2007. Molecular determinants of intrinsic multidrug resistance in cancer cells and tumors. In: Teicher, B. (Ed.), Cancer Drug Discovery and Development: Cancer Drug Resistance. Humana Press Inc., Totowa, N.J., pp. 241–260.

Nieman, J.A., Coleman, J.E., Wallace, D.J., Piers, E., Lim, L.Y., Roberge, M., Andersen, R.J., 2003. Synthesis and antimitotic/cytotoxic activity of hemiasterlin analogues. J. Nat. Prod. 66, 183–199.

Nunes, M., Kaplan, J., Wooters, J., Hari, M., Minnick Jr., A.A., May, M.K., Shi, C., Musto, S., Beyer, C., Krishnamurthy, G., Qiu, Y., Loganzo, F., Ayral-Kaloustian, S., Zask, A., Greenberger, L.M., 2005. Two photo affinity analogues of tripeptide, hemiasterlin, exclusively label alpha-tubulin. Biochemistry 44, 6844–6857.

Pal, D., Udata, C., Mitra, A.K., 2000. Transport of cosalane, a highly lipophilic novel anti-HIV agent, across Caco-2 cell monolayers. J. Pharm. Sci. 89, 826–833.

Pavan, B., Dalpiaz, A., 2011. Prodrugs and endogenous transporters: are they suitable for drug targeting into the central nervous system? Curr. Pharm. Des. 17, 3560–3576.

Pavan, B., Paganetto, G., Rossi, D., Dalpiaz, A., 2014. Multidrug resistance in cancer or inefficacy of neuroactive agents: innovative strategies to inhibit or circumvent the active efflux transporters selectively. Drug Discov. Today 19, 1563–1571.

Raje, S., Cao, J., Newman, A.H., Gao, H., Eddington, N.D., 2003. Evaluation of the blood-brain barrier transport, population pharmacokinetics, and brain distribution of benztropine analogs and cocaine using in vitro and in vivo techniques. J. Pharmacol. Exp. Ther. 307, 801–808.

Ravi, M., Zask, A., Rush, T.S., 2005. 3rd structure-based identification of the binding site for the hemiasterlin analogue HTI-286 on tubulin. Biochemistry 44, 15871–15879.

Roberti, M., Pizzirani, D., Simoni, D., Rondanin, R., Barucchello, R., Bonora, C., Buscemi, F., Grimaudo, S., Tolomeo, M., 2003. Synthesis and biological evaluation of resveratrol and analogues as apoptosis-inducing agents. J. Med. Chem. 46, 3546–3554.

Rothen-Rutishauser, B., Braun, A., Gunthert, M., Wunderli-Allenspach, H., 2000. Formation of multilayers in the caco-2 cell culture model: a confocal laser scanning microscopy study. Pharm. Res. 17, 460–465.

Simoni, D., Invidiata, F.P., Eleopra, M., Marchetti, P., Rondanin, R., Baruchello, R., Grisolia, G., Tripathi, A., Kellogg, G.E., Durrant, D., Lee, R.M., 2009. Design, synthesis and biological evaluation of novel stilbene-based antitumor agents. Bioorg. Med. Chem. 17, 512–522.

Simoni, D., Lee, R.M., Durrant, D.E., Chi, N.W., Baruchello, R., Rondanin, R., Rullo, C., Marchetti, P., 2010. Versatile synthesis of new cytotoxic agents structurally related to hemiasterlins. Bioorg. Med. Chem. Lett. 20, 3431–3435.

Valerii, M.C., Ricci, C., Spisni, E., Di Silvestro, R., De Fazio, L., Cavazza, E., Lanzini, A., Campieri, M., Dalpiaz, A., Pavan, B., Volta, U., Dinelli, G., 2015. Responses of peripheral blood mononucleated cells from non-celiac gluten sensitive patients to various cereal sources. Food Chem. 176, 167–174.

Wu, C.P., Hsieh, C.H., Wu, Y.S., 2011. The emergence of drug transporter-mediated multidrug resistance to cancer chemotherapy. Mol. Pharm. 8, 1996–2011.

Yee, S., 1997. In vitro permeability across Caco-2 cells (colonic) can predict in vivo (small intestine) absorption in man - fact or myth. Pharm. Res. 14, 763–766.

Yue, Q.X., Liu, X., Guo, D.A., 2010. Microtubule-binding natural products for cancer therapy. Planta Med. 11, 1037–1043.

Zask, A., Kaplan, J., Musto, S., Loganzo, F., 2005. Hybrids of the hemiasterlin analogue taltobulin and the dolastatins are potent antimicrotubule agents. J. Am. Chem. Soc. 127, 17667–17671.

Zhang, Z., Schwartz, S., Wagner, L., Miller, W., 2000. A greedy algorithm for aligning DNA sequences. J. Comput. Biol. 7, 203–214.